Nuclear Engineering and Technology 50 (2018) 432–438

Contents lists available at ScienceDirect

Nuclear Engineering and Technology

journal homepage: www.elsevier.com/locate/net

Original Article

Characterization of saturation of CR-39 detector at high alpha-particle fluence

M. El Ghazaly [a, b, *], Nabil M. Hassan [a, c]

[a] Department of Physics, Faculty of Science, Zagazig University, Zagazig, 44519, Egypt
[b] Department of Physiology, Faculty of Medicine, Taif University, Taif, 21974, Saudi Arabia
[c] Department of Natural Radiation Safety, Korea Institute of Nuclear Safety, 62, Gwahak-ro, Yuseong-gu, Daejeon, 34142, Republic of Korea

ARTICLE INFO

Article history:
Received 20 January 2017
Received in revised form
17 November 2017
Accepted 24 November 2017
Available online 18 December 2017

Keywords:
Alpha Particle
Bulk Etch Rate
CR-39 Detector
Saturated Regime
UV–Vis Spectroscopy

ABSTRACT

The occurrence of saturation in the CR-39 detector reduces and limits its detection dynamic range; nevertheless, this range could be extended using spectroscopic techniques and by measuring the net bulk rate of the saturated CR-39 detector surface. CR-39 detectors were irradiated by 1.5 MeV high alpha-particle fluence varying from 0.06×10^8 to 7.36×10^8 alphas/cm^2 from Am-241 source; thereafter, they were etched in a 6.25N NaOH solution at a temperature of 70°C for different durations. Net bulk etch rate measurement of the 1.5 MeV alpha-irradiated CR-39 detector surface revealed that rate increases with increasing etching time and reaches its maximum value at the end of the alpha-particle range. It is also correlated with the alpha-particle fluence. The measurements of UV–Visible (UV–Vis) absorbance at 500 and 600 nm reveal that the absorbance is linearly correlated with the fluence of alpha particles at the etching times of 2 and 4 hour. For extended etching times of 6, 10, and 14.5 hour, the absorbance is saturated for fluence values of 4.05×10^8, 5.30×10^8, and 7.36×10^8 alphas/cm^2. These new methods pave the way to extend the dynamic range of polymer-based solid state nuclear track detectors (SSNTDs) in measurement of high fluence of heavy ions as well as in radiation dosimetry.

1. Introduction

In the field of radiation dosimetry, poly allyl diglycol carbonate, CR-39 detector, is the most applicable detector in the solid state nuclear track detectors (SSNTDs) family because of its excellent optical properties [1,7,9,10,15]. Therefore, CR-39 detectors are used in various branches of science and technology, such as cosmic ray studies, radiation biology, radon monitoring, neutron radiography, particle identification, radiation dosimetry, X-rays reflectivity, and low linear energy transfer (LLET) radiation like ultraviolet and plasma detection [2–6,14,16,17,20–22]. In principle, CR-39 detector is insensitive to low doses of LLET radiation such as X-rays, gamma rays, and electrons [1,9]. CR-39 detectors have been preferred to detect perpendicularly incident heavy ions, with efficiency up to 100%; in some cases such as in high energy experiments, CR-39 detectors have been integrated with other types of detectors [1].

When the CR-39 detector is irradiated with heavy ions, permanent latent tracks are produced along their trajectories as a result of breaking of molecular bonds of the CR-39 detector's material while these ions lose their energies. The core radii of the latent tracks in the CR-39 detector are within several nanometers, depending on the heavy ion species and energies [1]. After chemical etching, the latent tracks are enlarged and visualized under an optical microscope as dark circles. For a low track density and a short etching time (tracks are not overlapped), track diameters or track profiles are counted with good detection efficiency up to 100% and with low systematic error [1]. However, in the case of a high track density and a long etching time, the tracks are overlapped in such a way that manual or automatic detection cannot distinguish individual tracks. Neither track density nor diameter can be precisely counted (saturation regime).

Fig. 1 shows the 1.5 MeV alpha-particle range in the CR-39 detector, calculated using the computer code SRIM [23,24]; the range amounts to 9 μm. All 1.5 MeV alpha particle that are incident perpendicular on the CR-39 detector surface will be detected since alpha particles are incident with an angle less than the critical angle. The energy deposited by the 1.5 MeV alpha particle is sufficient to dissociate all bonds in the CR-39 detector, even the strongest one –C=C– which has a dissociation energy of 6.4 eV [18].

* Corresponding author.
E-mail address: ghazaly2000@yahoo.com (M. El Ghazaly).

https://doi.org/10.1016/j.net.2017.11.010

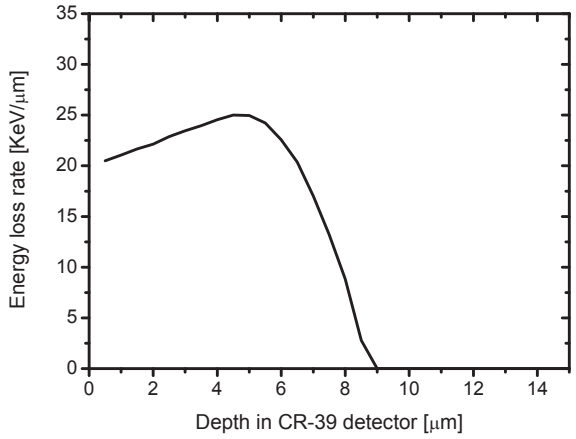

Fig. 1. Variation of the linear energy transfer (LET) as a function of the depth in CR-39 detector for alpha particle of 1.5 MeV [23,24].

Few studies have reported the utilization of the CR-39 detector in high-fluence applications. Zylstra et al. [25] reported a new model to account for track overlap in CR-39, which is limited to only two tracks. Rajta et al. [12] optimized the particle fluence in micromachining of CR-39 detector irradiated with proton and alpha particles. Yamauchi [19] deduced a model of the overlapping probability of latent and overlapped tracks. Gaillard et al. [8] studied the optical properties of the saturation of CR-39 detectors at high fluence. Rosenberg et al. [13] empirically determined the upper fluence limit for 100% detection efficiency of 2.4 MeV protons in CR-39 detectors and increased the maximum detection by using a pinhole and scattering foil with dimensions of several mm in front of the CR-39 detector; this method reduces proton fluence at the CR-39 detector by a factor of 50, resulting in an increase of the operating yield upper limit by a comparable amount.

Using different spectroscopic techniques including UV–Visible (UV–Vis) spectroscopy, the present work aims to explore the potential of the CR-39 detector to measure high alpha-particle fluence. The dependence of the UV-absorbance on both the alpha-particle fluence and the etching time is discussed in detail. A new formula to calculate the net bulk etch rate of an irradiated CR-39 detector surface is deduced. Correlation among the induced modifications in the bulk etch rate of the CR-39 detector with high alpha-particles fluence is reported.

2. Materials and methods

CR-39 detector sheet from Track Analysis System Ltd., UK (TASTRAK), of density 1.32 g/cm^3, refractive index for visible light 1.498, molecular composition $C_{12}H_{18}O_7$, and thickness 500 μm, was cut into pieces of 4 cm^2. CR-39 detectors were irradiated with alpha particles with energy of 1.5 MeV, emitted from a 9 μCi Am-241 source, which emits 5.48 MeV alpha particles. The irradiation was carried out in air at a distance from the source of 3.34 cm, which corresponds to alpha-particle energy of 1.5 MeV. The Am-241 alpha particle source was free from collimators, so as to ensure that the area of the target material (4 cm^2) was wholly irradiated. CR-39 detectors were irradiated with alpha fluences of 0.06 × 10^8, 0.07 × 10^8, 0.29 × 10^8, 1.47 × 10^8, 4.05 × 10^8, 5.30 × 10^8, and 7.36 × 10^8 alphas/cm^2. Then, CR-39 detectors were etched in a chemical solution of 6.25N NaOH at a temperature of 70 ± 1°C and for different periods of time. Bulk etch rate, the rate of removal of layers of the undamaged surface of CR-39, was determined using the mass decrement method. The UV–visible spectra were measured using a spectrophotometer (Model Spectro dual split beam, UVS-2700) at wavelengths in a range from 190 to 900 nm, keeping air as a reference. The calculated attenuation coefficient of the excitation wavelength of 290 nm in the CR-39 detector was 10.08 cm^{-1}. This means that, because of the alpha particle of energy of 1.5 MeV and range of 9 μm, the particles penetrate to a greater depth through the CR-39 detector, beyond the damage zone [23,24].

3. Results and discussion

3.1. Effect of high-fluence alpha particle on bulk etch rate of CR-39 detector

The bulk etch rate (V_B) of the CR-39 detector, which is the etching rate of the undamaged detector surface, can be determined using several methods such as the thickness decrement method, mass decrement method, and fission-fragment diameter method. In the current work, the bulk etch rate (V_B) was measured using the mass decrement method [10].

$$V_B = \frac{\Delta m}{2 t_e A \rho}, \tag{1}$$

where Δm is the mass decrement during the chemical etching of time of t_e (hour). A is the detector's surface area (cm^{-2}) and $\rho = 1.31$ g.cm^{-3} is the CR-39 detector material density. However, while the abovementioned method assumed that the bulk etch rate (V_B) over the whole surface of the detector is isotropic, this not the case: only one surface of the CR-39 detector was irradiated with a high fluence of alpha particles; this high fluence completely stopped within 9 μm of the exposed surface [23,24]. Therefore, rather than finding the true value of the specific surface, the measured bulk etch rate is averaged over the CR-39 detector surfaces. To deduce the correct bulk etch rate value at the high-fluence alpha-irradiated CR-39 detector, we assume $V_{B\alpha\text{-net}}$ is the measured bulk etch rate of the high-fluence alpha-irradiated CR-39 detector, and V_B is the bulk etching rate of the unexposed CR-39 detector surface. $V_{B\alpha}$ expresses simply the average value of the bulk etch rates for the exposed and nonexposed CR-39 detector surfaces. As a consequence, the measured etching rate of the alpha-irradiated CR-39 detector can be written in the following form:

$$V_{B\alpha} = \frac{V_{B\alpha-net} + V_B}{2}. \tag{2}$$

Then, the net bulk etch rate $V_{b\alpha\text{-net}}$ of the high-fluence alpha-irradiated CR-39 detector surface exposed to high-fluence alpha particles is determined by:

$$V_{B\alpha-net} = 2V_{B\alpha} - V_B. \tag{3}$$

However, this formula should be generalized and be available for application to any kind of radiation, in particular to ultraviolet radiation and heavy ions, absorbed in one surface of a solid state nuclear track detector, so as to allow the measurement of the correct value of the etching rate at an irradiated surface.

Fig. 2A presents the bulk etch rate of an unirradiated detector and the net bulk etch rate of the alpha particle-irradiated CR-39 detector. The bulk etch rate of the unirradiated CR-39 detector is determined using Eq. (1), while the bulk etch rate ($V_{B\alpha-net}$) of the alpha-irradiated CR-39 detector is determined by applying Eq. (3).

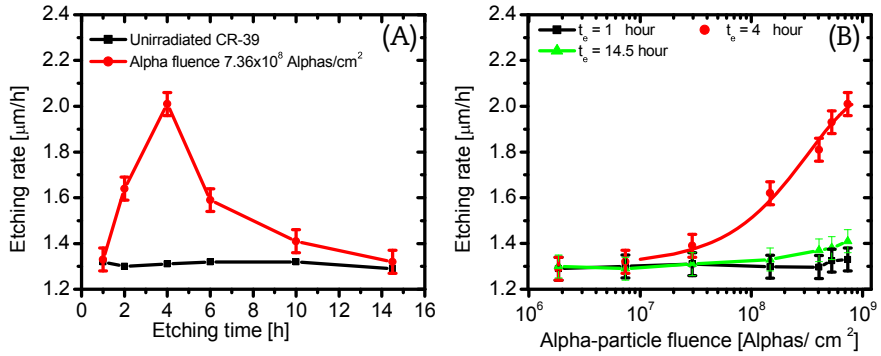

Fig. 2. (A) Bulk etching rate of unirradiated surface and for alpha-irradiated surface with fluence of 7.36×10^8 alphas/cm^2. (B) The dependence of the bulk etch rate on the fluence of alpha particle of 1.5 MeV at different etching times (all measurements are based on Eq. (4)).

It was observed that the bulk etch rate of the unirradiated CR-39 detector has a constant value of 1.29 ± 0.04 μm/hour over an etching time ranging from 1 to 14.5 hour, which is in agreement with the measurements reported in different works under the same etching conditions [1,10].

The net bulk etch rate ($V_{B\alpha-net}$) of the alpha-irradiated surface of the CR-39 detector increases with increasing etching time up to the maximum etching time of 4 hour, which corresponds to a removal thickness of about 8 μm, close to the range of the alpha particle with power of 1.5 MeV (9 μm) in the CR-39 detector. For a longer etching $t_e >> t_R$, where t_R is the time needed to etch the complete range of alpha particles in the CR-39 detector, the bulk etch rate decreases and goes back to the normal bulk etch rate (V_B) of the unirradiated surface of the CR-39 detector. In principle, the net bulk etch rate ($V_{B\alpha-net}$) of the alpha-irradiated surface of the CR-39 detector should follow the Bragg curve of energy loss depicted in Fig. 1. this is the case simply because $V_{B\alpha-net}$ reflects the damage induced by alpha particles in the CR-39 detector.

Fig. 2B, based on Eq. (4) as a function of the fluence of alpha particles with energy of 1.5 MeV at different etching times, illustrates the net bulk etch rate ($V_{B\alpha-net}$) of the alpha-irradiated surface of the CR-39 detector. Different characteristic points can be deduced from Fig. 2B; the net bulk etch rates for etching time of 1 h and 14.5 hour show a significant symmetry at nearly the same value, 2; the net etching rate of the exposed surface is increased by increasing of the alpha-particle fluence to about 2 μm/hour for an alpha fluence of 7.36×10^8 at an etching time of 4 hour. The net bulk etch rate increased by about 53.4% compared to that of the unirradiated surface, with a bulk etch rate of 1.29 ± 0.04 μm/hour. This increase in the net bulk etch rate is attributed to the energy deposited by the alpha particles on the CR-39 detector surface; this energy is capable of dissociating the chemical bonds of the carbonyl group C=O, which has a maximum binding energy of 8.281 eV [18]. This results in an acceleration of the net bulk etching rate of the irradiated surface of the CR-39 detector. In other words, the irradiated surface of the CR-39 detector, with high fluence of alpha particles, is almost etched at an etching rate the same as the track etch rate.

An empirical formula was deduced to describe the correlation between the alpha particle fluence f and the net bulk etching rate ($V_{B\alpha-net}$) of the alpha-irradiated surface of the CR-39 detector:

$$V_{B\alpha-net}(f) = 2.073 - 0.765Exp\left[\frac{-f}{2.23 \times 10^8}\right] \quad (4)$$

However, this equation is applicable only at the end of the charged particle range in the CR-39 detector, where the net bulk etch rate ($V_{B\alpha-net}$) is at its maximum.

3.2. Effect of alpha particle irradiation and chemical etching processes on the UV–Vis spectra

Three parameters control the probability of alpha particle tracks overlapping; these are alpha particle energy, etching time, and alpha-particle fluence. Concerning energy at short etching time, lower energy alpha particles produce tracks of larger diameters than do particles of higher energy. Tracks of larger diameters are more susceptible to overlap. Therefore, the CR-39 detector is saturated even for a lower track density. Yamauchi [19] derived a recurrence-relation model of monoenergetic tracks, the track occupation fraction A(n), as a function of ion fluence (n) particles/cm^2 for latent track of area (s) in the CR-39 detector.

$$A(n) = 1 - [1 - s]^n. \quad (5)$$

According to Eq. (5) for the chemical etched CR-39 detector, the opening area was significantly increased to several micrometers compared to the case of latent tracks, which are of several nanometers radius; the detector is fully occupied at lower fluence. For example, the surface of a CR-39 detector with an area of 1 cm^2 can be fully occupied with alpha-particle fluence of 7.96×10^{12} alphas/cm^2 for a latent track of radius of 2 nm, while the same surface area of another CR-39 detector was fully occupied with alpha-particle fluence of 7.96×10^6 alphas/cm^2 for a track radius of 2 μm.

Fig. 3 presents a photomicrograph of an irradiated CR-39 detector with different fluence values of alpha particles and etching for 4 hour in 6.25N NaOH solution at 70 ± 1°C; (a) Unirradiated CR-39 detector, (b) irradiated by fluence of 0.06×10^8 alphas/cm^2, (c) 0.07×10^8 alphas/cm^2, (d) 0.29×10^8 alphas/cm^2, (e)1.47×10^8 alphas/cm^2, (f) irradiated with 4.05×10^8 alphas/cm^2, (g) 5.30×10^8 alphas/cm^2, and (h) 7.36×10^8 alphas/cm^2. It was observed that, at the same etching time, alpha particle track overlap occurred when fluence increased.

Fig. 4 shows a photomicrograph of a CR-39 detector irradiated with alpha particle of energy of 1.5 MeV and fluence of 7.36×10^8 alphas/cm^2, etched in a chemical solution of 6.25N NaOH at 70 ± 1°C for different periods of time: (a) Unetched, (b) $t_e = 0.5$ hour, (c) $t_e = 1$ hour, (d) $t_e = 2$ hour, (e) $t_e = 4$ hour, (f) $t_e = 6$ hour, (g) $t_e = 10$ hour, and (h) $t_e = 14.5$ hour. For the same alpha-particle fluence, as the track diameter (size) increased with the chemical etching time, the unoccupied area vanished, as shown in Fig. 4E–4H. For a prolonged etching time of 4 hour or more, alpha tracks are completely overlapped and the unoccupied area completely disappeared. The overlapped tracks give rise to an increase of the opacity of the CR-39 detector due to an increase in the surface roughness, which causes significant light scattering.

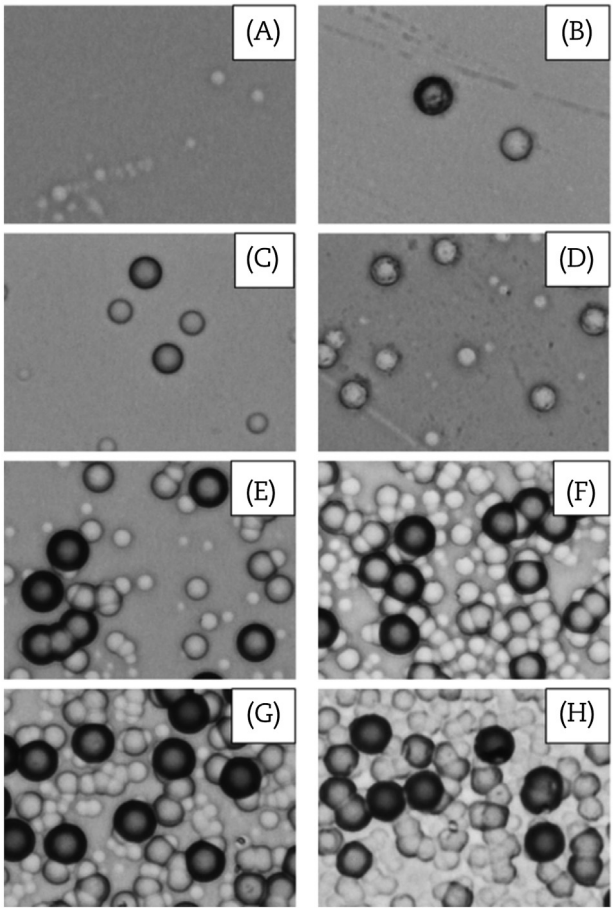

Fig. 3. Microscope images of the CR-39 detector irradiated with a different fluence of alpha particle and etched for 4 h in 6.25N NaOH at 70°C. (A) Unirradiated CR-39. (B) 0.06×10^8 alphas/cm^2. (C) 0.07×10^8 alphas/cm^2. (D) 0.29×10^8 alphas/cm^2. (E) 1.47×10^8 alphas/cm^2. (F) 4.05×10^8 alphas/cm^2. (G) 5.30×10^8 alphas/cm^2. (H) 7.36×10^8 alphas/cm^2. The frame area is 66.6×50 μm^2.

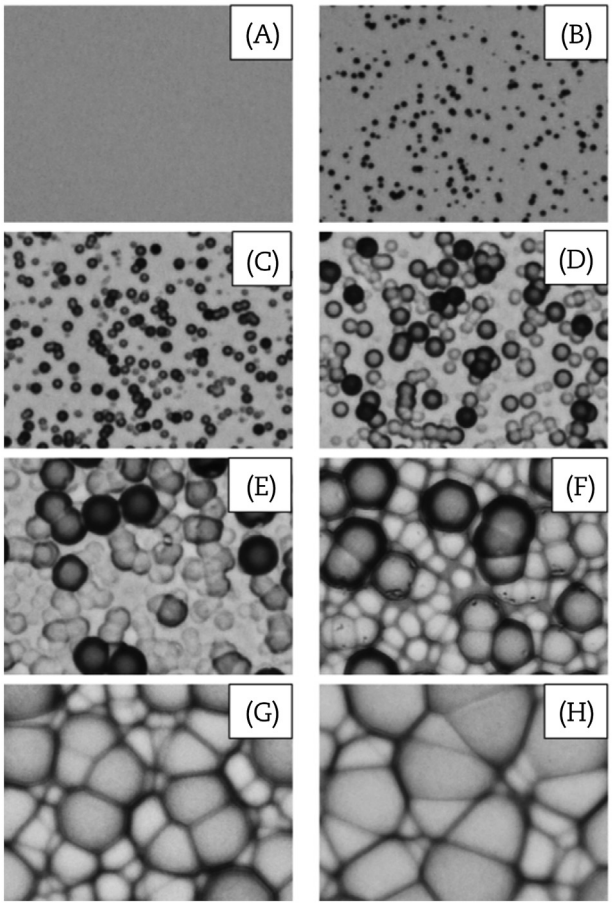

Fig. 4. Microscope images of CR-39 detector irradiated with alpha particle of energy 1.5 MeV and fluence of 7.36×10^8 alphas/cm^2 and etched in 6.25N NaOH at 70 ± 1°C for different etching times, (A) unetched. (B) $t_e = 0.5$ h. (C) $t_e = 1$ h. (D) $t_e = 2$ h. (E) $t_e = 4$ h. (F) $t_e = 6$ h. (G) $t_e = 10$ h. (H) $t_e = 14.5$ h. The frame area is 66.6×50 μm^2.

In principle, the light scattering by alpha particle tracks in the CR-39 detector is a strong function of the alpha particle track phase, including conical, transition, and spherical phases [11]. Conical phase occurs when $t_e < t_R$, see Fig. 4B and 4C; the track etch rate V_T is almost constant, and the alpha track profile is approximately triangular. However, at all points on the track surface, the light rays are totally internally reflected in the CR-39 detector and could not reach the detection hemisphere of the optical microscope [11]. Therefore, tracks appeared as completely dark circles for a perpendicular incident alpha particle.

A transition phase is present when $t_e \cong t_R$; the track etch rate V_T is increased because energy deposition by alpha particles increases. The alpha track profile is almost trapezoid, with a shorter parallel side inside the CR-39 detector and longer parallel side on the CR-39 detector surface. For the parallel side, the light goes through without scattering; however, the light is totally reflected at the alpha track wall. Therefore, alpha tracks appeared as concentric small bright circles and outer dark circles [11].

Spherical phase occurs when $t_e >> t_R$; the track etch rate vanishes because tracks move beyond the alpha particle range and the alpha track is spherical in shape. At the bottom surface, incoming light almost passes through, with a small refracted angle; the light intensity loss is relatively small. Consequently, the central part of the alpha track is bright. Moving away from the alpha track center, the gray level changes slightly and continually toward the peripheral area of the alpha opening. The light rays again are totally internally reflected, making an outer dark ring of the alpha particle track; see Fig. 4E–4H [11].

Fig. 5 presents the UV–Vis absorbance spectra of the alpha-irradiated CR-39 detector etched for 4 hour in 6.25N NaOH at 70°C for the following fluences: unirradiated CR-39, 0.06×10^8 alphas/cm^2, 0.07×10^8 alphas/cm^2, 0.29×10^8 alphas/cm^2, 1.47×10^8 alphas/cm^2, 4.05×10^8 alphas/cm^2, 5.30×10^8 alphas/cm^2, and 7.36×10^8 alphas/cm^2. It can be observed that the absorbance increases with increasing of the alpha-particle fluence incident on the CR-39 detector. For an etching time of 4 hour, the removal thickness is 5.16 μm for the unirradiated CR-39 detector. Therefore, the alpha particle tracks are in transition phase, where the light scattering is at a maximum. Consequently, the absorbance of light through the irradiated CR-39 detector increases. Furthermore, there is a clear red shift of the absorption edge, which is increased with increasing of the alpha-particle fluence.

Fig. 6A shows the UV–Vis absorbance spectra of the unirradiated CR-39 detector at different etching times. Fig. 6B depicts the absorbance at two wavelengths, 500 and 600 nm, as a function of the etching time. UV–Vis absorbance of the CR-39 detector increased by about 87% from 0.039 to 0.073, which is insignificant because 0.073 is a negligible absorbance. However, this slight increase in absorbance may be attributed either to the increase in the surface roughness of the CR-39 detector or to a formation of a thin bi-product layer on the CR-39 detector surface by the chemical

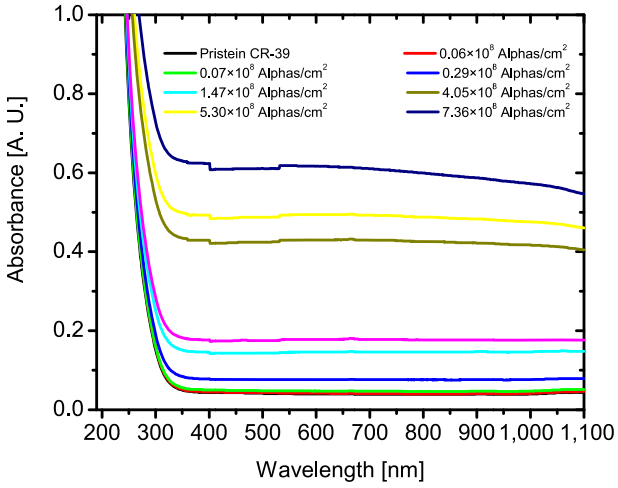

Fig. 5. UV–Vis spectra of alpha-irradiated CR-39 detector of different fluence, etched for 4 h in 6.25N NaOH solution at 70 ± 1°C.

etching, which increases the absorbance. The absorption edges were determined as a function of the etching time from the UV–Vis spectra; these edges were found to be constant at 322 ± 5 nm and did not show significant correlation with the etching time of the unirradiated CR-39 detector. However, this indicates that chemical etching of the CR-39 detector in 6.25N NaOH at 70°C maintains the optical properties of the CR-39 detector. The absorbance-etching time data are fitted using the linear equation:

$$Abs(t_e) = 0.04 + 0.0025\ t_e \quad (6)$$

The rate of absorbance change with respect to etching time is 0.0025, which is negligible and shows the stability of the optical properties of the CR-39 detector under chemical etching for long duration at a temperature of 70°C.

Fig. 7A presents the UV–Vis spectra of the CR-39 detector irradiated with alpha particles with energy of 1.5 MeV and fluence of 7.36×10^8 alphas/cm^2, etched in 6.25N NaOH at a temperature of 70°C for different durations. The absorbance increased with increasing of the etching time up to 6 hour; it then decreases as the etching time proceeds to 10 and 14 hour, as shown in Fig. 7B. This behavior can be explained by the increase of the roughness of the alpha-irradiated CR-39 detector surface before the end of the range of the 1.5 MeV alpha particles, which amounts to 9 μm. As the chemical etching proceeds, the alpha track phase changes from conical, in which the light scattering is maximum, to transition, in which the scattering of light is moderate, and further to spherical, in which the light scattering is at a minimum. However, for the etching time $t_e >> t_R$, the chemical etching reduces the roughness of the irradiated CR-39 detector surface, giving rise to a reduction in the light scattering and to an absorbance decrease in the CR-39 detector. Fig. 7B presents the absorbance *Abs* (t_e) at 500 and 600 nm (visible light spectra); the data are fitted with the following function:

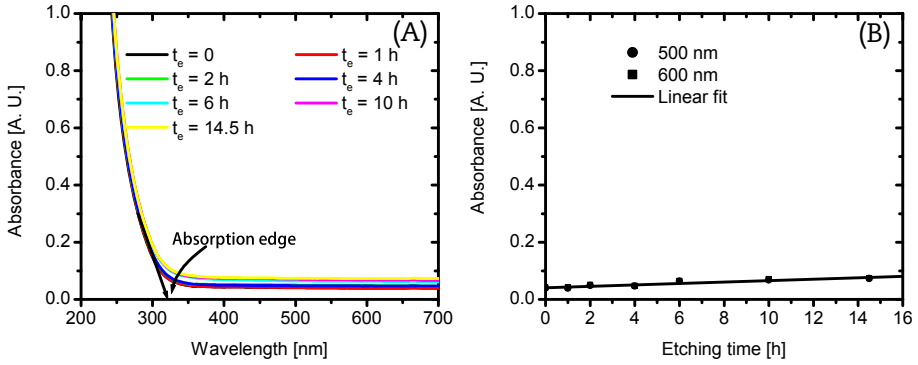

Fig. 6. (A) UV–Vis spectra of the unirradiated CR-39 detector etched in 6.25N NaOH solution at 70 ± 1°C for different duration. (B) The absorption of the unirradiated CR-39 detector at 500 and 600 nm.

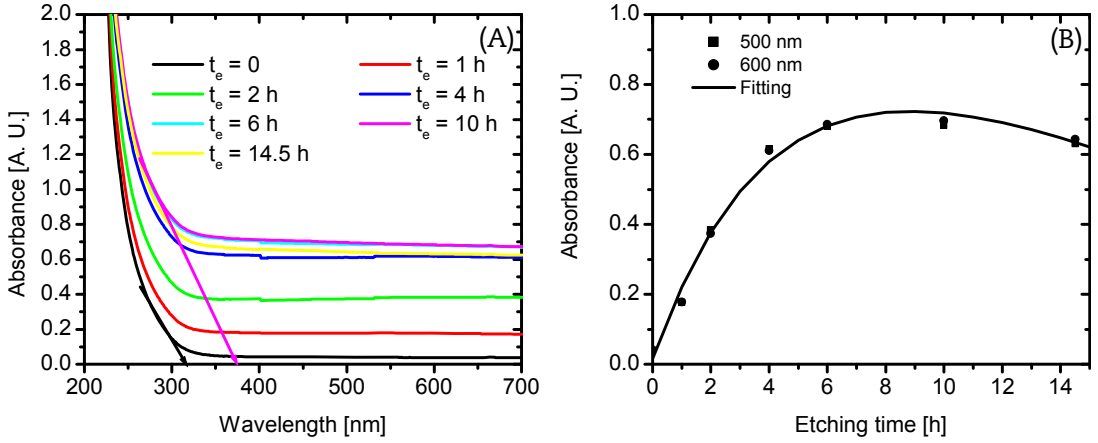

Fig. 7. (A) UV–Vis spectra of the CR-39 detector irradiated with alpha particle of energy 1.5 MeV and fluence 7.36×10^8 alphas/cm^2 etched in 6.25N NaOH at a temperature of 70°C for different durations. (B) The absorption of unirradiated CR-39 as a function of etching time at 500 and 600 nm.

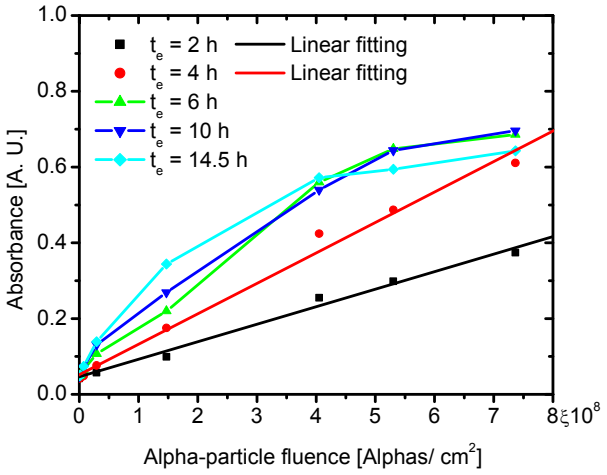

Fig. 8. The absorption spectra at 500 nm of the CR-39 irradiated detector with alpha particle of energy 1.5 MeV as a function of alpha particle fluence, CR-39 detector is chemically etched in 6.25N NaOH solution at 70 ± 1°C for different durations.

$$Abs(t_e) = 1.97 - 0.36t_e - 118\ Exp[-0.23t_e] \quad (7)$$

From the UV–Vis spectra, the absorption edges were measured as a function of the etching time. The absorption edge of the un-irradiated CR-39 detector is 319 ± 5 nm; this value increases with increasing of the etching time and reaches a value of 373 ± 5 nm. However, this indicates that the chemical etching of the alpha-irradiated CR-39 detector in 6.25N NaOH at 70°C induces slight modifications in the detector's optical properties at the absorption edge.

Fig. 8 presents the absorbance at 500 nm of the irradiated CR-39 detector with alpha particle of energy 1.5 MeV as a function of alpha particle fluence; CR-39 detector is chemically etched in 6.25N NaOH at 70°C for different durations. For etching times of 2 and 4 hour, there is a linear relationship between alpha-particle fluence and absorbance at 500 nm; data are fitted using the following linear function:

$$Abs(F) = a_1 + b_1F \quad (8)$$

where $a_1 = 0.046$ and $b_1 = 4.6 \times 10^{10}$ are fitting parameters; R = 99.6, with standard deviation of 0.013, and $p < 0.0001$ for a chemical etching time of 2 hour. For 4 hour chemical etching, $a_1 = 0.051$, $b_1 = 8.1 \times 10^{10}$, and R = 99.5, with standard deviation of 0.025 and $p < 0.0001$. The linear curves obtained between the absorbance and alpha-particle fluence can be used as calibration curves to determine the unknown high fluence of the alpha particles.

For prolonged etching times, starting from 6 hour, there is a trend of absorbance saturation in the CR-39 detector for alpha-particle fluences of 4.05×10^8, 5.30×10^8, and 7.36×10^8 alphas/cm^2.

4. Conclusion

In the present work, the characterization of a saturated CR-39 detector, irradiated with 1.5 MeV alpha particles, was carried out by measuring the net bulk etch rate and optical absorbance of the irradiated CR-39 detector. The applied net bulk etch rate of the alpha-irradiated CR-39 detector surface was determined by a new equation, $V_{B\alpha-net} = 2V_{B\alpha} - V_B$, derived using a simple theory. The net bulk etch rate measurement of the 1.5 MeV alpha-irradiated CR-39 detector surface revealed that this rate increases at the end of the alpha particle range and decreases after the alpha particle range. Furthermore, this behavior is correlated exponentially with the alpha-particle fluence. The light absorbance values at 500 and 600 nm are linearly correlated with the fluence of alpha particles at the etching times of 2 and 4 hour, which extend by many orders of magnitude the upper alpha-particle fluence. Extended etching times reduce the upper detection limit of the CR-39 detector, as revealed for etching times of 6, 10, and 14.5 hour; the absorbance is saturated for fluence values of 4.05×10^8, 5.30×10^8, and 7.36×10^8 alphas cm^{-2}. The obtained results pave the way to extending the dynamic range of CR-39 detector applications in radiation dosimetry of heavy ions as well as in LLET radiation.

Conflict of interest

We have no conflict of interest to declare.

Appendix A. Supplementary data

Supplementary data related to this article can be found at https://doi.org/10.1016/j.net.2017.11.010.

References

[1] S.A. Durrani, R.K. Bull, Solid State Nuclear Track Detection, Principles, Methods and Applications, Pergamon Press, 1987.
[2] M. El Ghazaly, On the X-ray reflectivity by poly allyl diglycol carbonate (PADC), J. Korean Phys. Soc. 59 (1) (2011) 55–58.
[3] M. El Ghazaly, On alpha particle spectroscopy based on the over-etched track length in PADC (CR-39 detector), Radiat. Eff. Def. Solids 167 (6) (2012) 421–427.
[4] M. El Ghazaly, T.T. Salama, E.I. Khalil, Kh.M. Abd El Raouf, Comparison between different models for alpha-particle range determination and a new approach to CR-39 detector, J. Korean Phys. Soc. 61 (6) (2012) 336–341.
[5] M. El Ghazaly, H.E. Hassan, Spectroscopic studies on alpha particle-irradiated PADC (CR-39 detector), Res. Phys. 4 (2014) 40–43.
[6] D. Fink, V. Hnatowicz, Fundamentals of ion-irradiated polymers, Springer Verlag, Berlin, Germany, 2007.
[7] R.L. Fleischer, P.B. Price, R.M. Walker, Nuclear Tracks in Solids: Principles and Applications, University of California Press, Berkeley, 1975.
[8] S. Gaillard, J.N. Fuchs, R.-L. Galloudec, T.E. Cowan, Study of saturation of CR39 nuclear track detectors at high ion fluence and of associated artifact patterns, Rev. Sci. Inst. 78 (2007) 013304.
[9] S. Manzoor, I.E. Qureshi, M.A. Rana, M.I. Shahzad, G. Sher, M. Sajid, H.A. Khan, G. Giacomelli, M. Giorgini, G. Mandrioli, L. Patrizii, V. Popa, P. Serra, V. Togo, Charge identification in CR-39 nuclear track detector using relativistic lead ion fragmentation, Nucl. Inst. Methods A 453 (2000) 525–529.
[10] D. Nikezic, K.N. Yu, Formation and growth of tracks in nuclear track materials, Mater. Sci. Eng. 46 (2004) 51–123.
[11] D. Nikezic, K.N. Yu, Analyses of light scattered from etched alpha-particle tracks in PADC, Radiat. Meas. 43 (2008) 1417–1422.
[12] I. Rajta, E. Baradács, A.A. Bettiol, I. Csige, K. Tőkési, L. Budai, A.Z. Kiss, Optimization of particle fluence in micromachining of CR-39, Nucl. Inst. Methods Phys. Res. B 231 (2005) 384–388.
[13] M.J. Rosenberg, F.H. Séguin, C.J. Waugh, H.G. Rinderknecht, D. Orozco, J.A. Frenje, M. Gatu Johnson, H. Sio, A.B. Zylstra, N. Sinenian, C.K. Li, R.D. Petrasso, S. LePape, A.J. Mackinnon, R.M. Bionta, O.L. Landen, R.A. Zacharias, Y. Kim, H.W. Herrmann, J.D. Kilkenny, A. Nikroo, A compact proton spectrometer for measurement of the absolute DD proton spectrum from which yield and ρR are determined in thin-shell inertial-confinement-fusion implosion, Rev. Sci. Inst. 85 (4) (2014) 043302.
[14] A.F. Saad, N.M. Al-Faitory, M. Hussein, R.A. Mohamed, Ultraviolet radiation-induced modifications of the optical and registration properties of a CR-39 nuclear track detector, Nucl. Inst. Methods B 359 (2015) 131–136.
[15] F.H. Séguin, J.A. Frenje, C.K. Li, D.G. Hicks, S. Kurebayashi, J.R. Rygg, B.-E. Schwartz, R.D. Petrasso, S. Roberts, J.M. Soures, D.D. Meyerhofer, T.C. Sangster, J.P. Knauer, C. Sorce, V. Glebov, Yu, C. Stoeckl, T.W. Phillips, R.J. Leeper, K. Fletcher, S. Padalino, Spectrometry of charged particles from inertial-confinement-fusion plasmas, Rev. Sci. Inst. 74 (2003) 975–995.
[16] Shang Bing, CR39 radon detector, Nucl. Tracks Radiat. Meas. 22 (1–4) (1993) 451–454.
[17] M.A. Stanojev Pereira, J.G.R. Marques, J.P. Santos, Improved track-etch neutron radiography using CR-39, Nucl. Inst. Methods A 764 (2014) 310–316.
[18] Uni-Waterloo, 2016. http://www.science.uwaterloo.ca/~cchieh/cact/c120/bondel.html. (Accessed 3 September 2015).
[19] T. Yamauchi, Studies on the nuclear tracks in CR-39 plastics, Radiat. Meas. 36 (73) (2003) 73–81.
[20] T. Yamauchi, D. Mineyama, H. Nakai, K. Oda, N. Yasuda, Track core size estimation in CR-39 track detector using atomic force microscope and UV–visible spectrophotometer, Nucl. Inst. Methods B 208 (2003) 149–154.

[21] K.N. Yu, D. Nikezic, F.M.F. Ng, J.K.C. Leung, Long term measurements of radon progeny concentrations with solid-state nuclear track detectors, Radiat. Meas. 40 (2005) 560–568.
[22] D. Zhou, D. O'Sullivan, E. Semones, M. Weyland, Charge spectra of cosmic ray nuclei measured with CR-39 detectors in low earth orbit, Nucl. Inst. Methods A 564 (1) (2006) 262–266.
[23] J.F. Ziegler, SRIM-2010. http://www.srim.org. (Accessed 3 November 2015).
[24] J.F. Ziegler, J.P. Biersack, U. Littmark, The Stopping and Range of Ions in Solids, Pergamon Press, New York, 1985.
[25] A.B. Zylstra, J.A. Frenje, F.H. Séguin, M.G. Johnson, D.T. Casey, M.J. Rosenberg, C. Waugh, N. Sinenian, M.J.E. Manuel, C.K. Li, R.D. Petrasso, Y. Kim, H.W. Herrmann, A new model to account for track overlap in CR-39 data, Nucl. Inst. Methods Phy. Res. A 681 (2012) 84–90.